# Validation of a new anisotropic yield criterion through bulge test

Prof. Dr.-Ing. D. Banabic, Dipl.-Ing. G. A. Cosovici, Dipl.-Ing. D.S. Comsa
Technical University of Cluj-Napoca, Romania


Dr.-Ing. S. Wagner, Prof. Dr. –Ing. K. Siegert
Institute for Metal Forming Technology, University of Stuttgart, Germany

## Abstract

The paper presents a new anisotropic yield criterion and its implementation in the ABAQUS/Standard finite-element code. The yield criterion is an extension of the formulation proposed by Barlat and Lian in 1989. In order to obtain a better representation of the plastic behaviour of the orthotropic sheet metals, some additional coefficients have been included in the expression of the equivalent stress. The constitutive model has been used in the simulation of a hydraulic bulging process. The numerical results have been compared with experimental data.

## 1 Introduction

The mechanics of the sheet metal forming processes is greatly influenced by the plastic anisotropy of the material. In order to obtain a proper description of the anisotropy, the classical von Mises yield criterion should be modified. Hill proposed in 1948 /1/ a simple anisotropic yield criterion in the form of a quadratic function. Since then, several scientists have developed more and more sophisticated yield functions for anisotropic materials. Hill himself successively improved his criterion in 1979, 1990 and 1993 /2, 3, 4/. Hosford /5/ initiated another interesting research direction by introducing an isotropic yield function based on crystallographic calculations. He also succeeded in extending this criterion to anisotropy /6/. During the last two decades, many other yield functions have been proposed aiming to improve the fitting with experimental data. Among the recent achievements in this field, one may notice the formulations proposed by Barlat and Lian /7/, Barlat et al. /8, 9, 10/, Karafillis and Boyce /11/, as well as Cazacu and Barlat /12/. A comprehensive description of the most important yield criteria can be found in /13/.

The yield criterion used in this paper has been derived from the one proposed by Barlat and Lian /7/. The new coefficients included in the expression of the equivalent stress improve its capability to represent the anisotropy of sheet metals. The identification procedure needs seven material parameters: the uniaxial yield stresses and the coefficients of plastic anisotropy associated to three planar directions (defined by an angle of 0, 45 and 90° measured from the rolling direction), as well as the equibiaxial yield stress associated to the rolling and transverse directions.

The authors have included the new yield criterion into an elastoplastic constitutive model for membranes under plane-stress conditions. The constitutive model has been implemented as a UMAT subroutine in ABAQUS/Standard. The numerical simulation of a hydraulic bulging process has been performed in order to evaluate the performances of the model.

## 2  Description of the new yield criterion

### 2.1  Equation of the yield surface

A yield surface is generally described by an implicit equation having the form

$$\Phi(\overline{\sigma}, Y) := \overline{\sigma} - Y = 0 \tag{1}$$

where $\overline{\sigma}$ is the equivalent stress and Y is a yield parameter. The sheet metal is assumed to behave as an orthotropic membrane under plane-stress conditions. Using this hypothesis, the equivalent stress is defined as follows:

$$\overline{\sigma} = \left[ a(\Gamma + \Psi)^{2k} + a(\Gamma - \Psi)^{2k} + (1 - a)(2\Psi)^{2k} \right]^{\frac{1}{2k}} \tag{2}$$

where $0 \le a \le 1$ and $k \in N^*$ are material parameters, while $\Gamma$ and $\Psi$ are functions depending on the non-zero components of the stress tensor:

$$\Gamma = M\hat{\sigma}_{11} + N\hat{\sigma}_{22}, \quad \Psi = \sqrt{\left(P\hat{\sigma}_{11} - Q\hat{\sigma}_{22}\right)^2 + R^2\hat{\sigma}_{12}\hat{\sigma}_{21}} \tag{3}$$

The coefficients M, N, P, Q and R in equation (3) are also material parameters. The stress components $\hat{\sigma}_{\alpha\beta}$ $(\alpha, \beta = 1,2)$ are expressed in an orthonormal basis coincident with the axes of plastic orthotropy (1 is the rolling direction – RD, 2 is the transverse direction – TD, while 3 is the normal direction – ND).

One may prove that the yield surface defined by equations (1) – (3) is always convex in the stress space if $0 \le a \le 1$ and k is a strictly positive integer number.

The shape of the yield surface is controlled by seven material parameters: k, a, M, N, P, Q and R. The integer exponent k has a special status. Its value is established in accordance with the crystallographic structure of the material /5/:

$\quad$ k = 3 $\qquad\qquad$ for BCC alloys

$\quad$ k = 4 $\qquad\qquad$ for FCC alloys.

The other six parameters (a, M, N, P, Q and R) are established in such a way that the constitutive equations associated to the yield surface reproduce as well as possible the plastic behaviour of the sheet metal. The identification procedure is described in §2.4.

One may notice that the equivalent stress defined by equations (2) – (3) is very similar to the expression proposed by Barlat and Lian /7/ for orthotropic sheet metals under plane-stress conditions. In fact, the Barlat-Lian formulation may be obtained assigning particular values to the coefficients M, N, P, Q and R.

## 2.2　Flow rule

The flow rule associated to the yield surface described by equations (1) – (3) is /14/

$$\dot{\varepsilon}^p_{\alpha\beta} = \dot{\bar{\varepsilon}}^p \frac{\partial\Phi}{\partial\hat{\sigma}_{\alpha\beta}}, \quad \alpha,\beta = 1,2 \tag{4}$$

where $\dot{\varepsilon}^p_{\alpha\beta}(\alpha,\beta = 1,2)$ are the planar components of the plastic strain-rate tensor (also expressed in the system of orthotropy axes), and $\dot{\bar{\varepsilon}}^p$ is the equivalent plastic strain-rate. The last quantity is defined by the power law

$$\bar{\sigma}\dot{\bar{\varepsilon}}^p = \hat{\sigma}_{\alpha\beta}\dot{\varepsilon}^p_{\alpha\beta} \tag{5}$$

Here and in the subsequent equations, the tensor summation rule is used (the Greek indices take the values 1 and 2, while the Latin ones take the values 1, 2 and 3).

The non-planar components of the plastic strain-rate tensor are restricted by the plane-stress condition for membranes and the isochoric character of the plastic deformation:

$$\dot{\varepsilon}^p_{\alpha 3} = \dot{\varepsilon}^p_{3\alpha} = 0, \quad \alpha = 1,2$$
$$\dot{\varepsilon}^p_{33} = -\dot{\varepsilon}^p_{\gamma\gamma} \tag{6}$$

## 2.3　Hardening law

Assuming a purely isotropic hardening of the sheet metal, only one scalar parameter is needed for describing the evolution of the yield surface. This is the so-called plastic equivalent strain computed as the time-integral of the equivalent plastic strain-rate:

$$\overline{\varepsilon}^p = \int_0^T \dot{\overline{\varepsilon}}^p \, dt \tag{7}$$

The evolution of the yield surface has been taken into account by means of a Swift hardening law /14/:

$$Y(\overline{\varepsilon}^p) = K(\varepsilon^0 + \overline{\varepsilon}^p)^n \tag{8}$$

where Y is the yield parameter (see equation (1)), while K, $\overline{\varepsilon}^0$ and n are material parameters. In this formulation, Y is chosen to be the uniaxial yield stress associated to the rolling direction.

## 2.4  Identification procedure

The parameters a, M, N, P, Q and R in the expression of the equivalent stress are computed in such a way that the constitutive equations associated to the yield surface reproduce as well as possible the following characteristics of the sheet metal:

$\sigma_0^{exp}$      yield stress obtained by a uniaxial tensile test along RD

$\sigma_{90}^{exp}$      yield stress obtained by a uniaxial tensile test along TD

$\sigma_{45}^{exp}$      yield stress obtained by a uniaxial tensile test along a direction equally inclined to RD and TD

$\sigma_b^{exp}$      yield stress obtained by an equibiaxial tensile test along RD and TD

$r_0^{exp}$      coefficient of plastic anisotropy associated to RD

$r_{90}^{exp}$      coefficient of plastic anisotropy associated to TD

$r_{45}^{exp}$      coefficient of plastic anisotropy associated to a direction equally inclined to RD and TD.

One may notice that seven conditions act on six material coefficients. Due to this over-constraint, the authors have adopted an identification procedure based on the minimisation of the following error-function:

$$f(a, M, N, P, Q, R) = \left(\frac{\sigma_0}{\sigma_0^{exp}} - 1\right)^2 + \left(\frac{\sigma_{90}}{\sigma_{90}^{exp}} - 1\right)^2 + \left(\frac{\sigma_{45}}{\sigma_{45}^{exp}} - 1\right)^2 + \left(\frac{\sigma_b}{\sigma_b^{exp}} - 1\right)^2 +$$
$$\left(\frac{r_0}{r_0^{exp}} - 1\right)^2 + \left(\frac{r_{90}}{r_{90}^{exp}} - 1\right)^2 + \left(\frac{r_{45}}{r_{45}^{exp}} - 1\right)^2 \tag{9}$$

where $\sigma_0, \sigma_{90}, \sigma_{45}, \sigma_b, r_0, r_{90}$ and $r_{45}$ are the uniaxial yield stresses, the equibiaxial yield stress and the coefficients of plastic anisotropy predicted by the constitutive equations. The identification procedure needs formulas for evaluating these quantities.

### 2.4.1  Prediction of the uniaxial yield stress

Let $\sigma_\varphi$ be the uniaxial yield stress associated to a direction inclined at an angle $0° \leq \varphi \leq 90°$ to RD. The corresponding non-zero components of the stress tensor are

$$\hat{\sigma}_{11} = \sigma_\varphi \cos^2 \varphi, \quad \hat{\sigma}_{22} = \sigma_\varphi \sin^2 \varphi,$$
$$\hat{\sigma}_{12} = \hat{\sigma}_{21} = \sigma_\varphi \sin \varphi \cos \varphi \tag{10}$$

Equations (1) – (3) and (10) lead to the following formula for the uniaxial yield stress:

$$\sigma_\varphi = Y\!\big/\!F(\varphi) \tag{11}$$

where

$$F(\varphi) = \left[ a\left(\Gamma_\varphi + \Psi_\varphi\right)^{2k} + a\left(\Gamma_\varphi - \Psi_\varphi\right)^{2k} + (1-a)\left(2\Psi_\varphi\right)^{2k} \right]^{\frac{1}{2k}} \tag{12}$$

and

$$\Gamma_\varphi = M \cos^2 \varphi + N \sin^2 \varphi,$$
$$\Psi_\varphi = \sqrt{\left(P \cos^2 \varphi - Q \sin^2 \varphi\right)^2 + R^2 \sin^2 \varphi \cos^2 \varphi} \tag{13}$$

### 2.4.2  Prediction of the equibiaxial yield stress

In case of an equibiaxial tension along RD and TD, the planar components of the stress tensor are

$$\hat{\sigma}_{11} = \hat{\sigma}_{22} = \sigma_b, \quad \hat{\sigma}_{12} = \hat{\sigma}_{21} = 0 \tag{14}$$

Equations (1) – (3) and (14) lead to a formula for evaluating the equibiaxial yield stress:

$$\sigma_b = Y\!\big/\!F_b \tag{15}$$

where

$$F_b = \left[ a\left(\Gamma_b + \Psi_b\right)^{2k} + a\left(\Gamma_b - \Psi_b\right)^{2k} + (1-a)\left(2\Psi_b\right)^{2k} \right]^{\frac{1}{2k}} \tag{16}$$

and

$$\Gamma_b = M + N, \quad \Psi_b = |P - Q| \tag{17}$$

### 2.4.3  Prediction of the r-coefficient

The r-coefficient associated to a direction inclined at an angle $0° \leq \varphi \leq 90°$ to RD is defined as follows:

$$r_\varphi = \frac{\dot{\varepsilon}^p_{\varphi+90}}{\dot{\varepsilon}^p_{ND}} \tag{18}$$

where $\dot{\varepsilon}^p_{\varphi+90}$ is the planar component of the plastic strain-rate tensor associated to a direction inclined at $\varphi+90°$ to RD, and $\dot{\varepsilon}^p_{ND}$ is the component of the same tensor associated to ND. After using the condition of plastic incompressibility

$$\dot{\varepsilon}^p_\varphi + \dot{\varepsilon}^p_{\varphi+90} + \dot{\varepsilon}^p_{ND} = 0 \tag{19}$$

Equation (18) becomes

$$r_\varphi = -\frac{\dot{\varepsilon}^p_\varphi}{\dot{\varepsilon}^p_{ND}} - 1 \tag{20}$$

where $\dot{\varepsilon}^p_\varphi$ is the component of the plastic strain-rate tensor associated to the direction inclined at the angle $\varphi$ to RD. $\dot{\varepsilon}^p_\varphi$ and $\dot{\varepsilon}^p_{ND}$ may be rewritten using the tensor components expressed in the system of orthotropy axes:

$$\dot{\varepsilon}^p_\varphi = \dot{\hat{\varepsilon}}^p_{11} \cos^2\varphi + \dot{\hat{\varepsilon}}^p_{22} \sin^2\varphi + \dot{\hat{\varepsilon}}^p_{12} \sin\varphi\cos\varphi + \dot{\hat{\varepsilon}}^p_{21} \sin\varphi\cos\varphi,$$
$$\dot{\varepsilon}^p_{ND} = \dot{\hat{\varepsilon}}^p_{33} = -\dot{\hat{\varepsilon}}^p_{11} - \dot{\hat{\varepsilon}}^p_{22} \tag{21}$$

Because the r-coefficient is also defined for a uniaxial stress state, equations (10) are valid. It is then possible to write

$$\cos^2\varphi = \frac{\hat{\sigma}_{11}}{\sigma_\varphi}, \quad \sin^2\varphi = \frac{\hat{\sigma}_{22}}{\sigma_\varphi}, \quad \sin\varphi\cos\varphi = \frac{\hat{\sigma}_{12}}{\sigma_\varphi} = \frac{\hat{\sigma}_{21}}{\sigma_\varphi} \tag{22}$$

Equations (20) – (22), (1) – (5), and (11) – (13) lead to the desired formula for evaluating the coefficient of plastic anisotropy:

$$r_\varphi = \frac{[F(\varphi)]^{2k}}{G(\varphi)} - 1 \tag{23}$$

where

$$G(\varphi) = \left[a(\Gamma_\varphi + \Psi_\varphi)^{2k-1} + a(\Gamma_\varphi - \Psi_\varphi)^{2k-1}\right](M+N) + \left[a(\Gamma_\varphi + \Psi_\varphi)^{2k-1} - a(\Gamma_\varphi - \Psi_\varphi)^{2k-1} + \right.$$
$$\left. 2(1-a)(2\Psi_\varphi)^{2k-1}\right]\frac{(P-Q)(P\cos^2\varphi - Q\sin^2\varphi)}{\Psi_\varphi} \tag{24}$$

The identification procedure uses equations (11) – (13), (15) – (17) and (23) – (24) to compute $\sigma_0, \sigma_{90}, \sigma_{45}, \sigma_b, r_0, r_{90}$ and $r_{45}$. Due to the complexity of these formulas, the authors have developed a numerical minimisation strategy based on the downhill simplex method /15/.

## 2.5  Numerical results of the identification procedure

The identification procedure has been tested for an alluminium alloy (AA3003-0, thickness 1 mm). The mechanical parameters used as input data are listed in Table 1:

| Mechanical parameters | AA3003-0 (thickness 1 mm) |
|---|---|
| $\sigma_0^{exp}$ | 57 MPa |
| $\sigma_{90}^{exp}$ | 55.6 MPa |
| $\sigma_{45}^{exp}$ | 57.5 MPa |
| $\sigma_b^{exp}$ | 58.5 MPa |
| $r_0^{exp}$ | 0.848 |
| $r_{90}^{exp}$ | 0.796 |
| $r_{45}^{exp}$ | 0.875 |

Table. 1   Mechanical parameters of an aluminium alloy (AA3003-0)

Table 2 shows the coefficients provided by the identification procedure. The corresponding values of the parameters k and Y are also presented.

| Coefficients of the yield criterion | AA3003-0 (thickness 1 mm) |
|---|---|
| A | 0.6576 |
| M | 0.4676 |
| N | 0.4735 |
| P | 0.5077 |
| Q | 0.5223 |
| R | 1.0426 |
| k | 4 |
| Y | 57 MPa |

Table. 2   Coefficients of the yield criterion aluminium alloy (AA3003-0)

These coefficients will be input data for the numerical simulation of a hydraulic bulging test.

## 2.6  Mechanical model of a hydraulic bulging test

The sheet metal subjected to hydraulic bulging is assumed to behave as an elastoplastic membrane under plane-stress conditions. The elastic component of the strain is generally very small as compared to the plastic part, while the rotations of the material volumes are large. Due to the small amount of elastic deformation, the incompressibility condition is used when updating the thickness of the membrane. A linearly isotropic constitutive model describes the elastic behaviour of the sheet metal. On the other hand, its plastic behaviour is assumed to be orthotropic. The local axes of plastic orthotropy change continuously during the forming process (their current orientation is given by the rotational component of the deformation gradient tensor). The new yield criterion, its associated flow rule and the Swift hardening law presented in §2 describe the plastic behaviour of the sheet metal.

A global coordinate system is used to express the current positions of the particles belonging to the membrane, as well as the external loads (generated by pressure in case of a hydraulic bulging process). Its unit vectors (denoted by $\mathbf{e}^1$, $\mathbf{e}^2$, $\mathbf{e}^3$ in Figure 1) are parallel to the initial axis of plastic orthotropy.
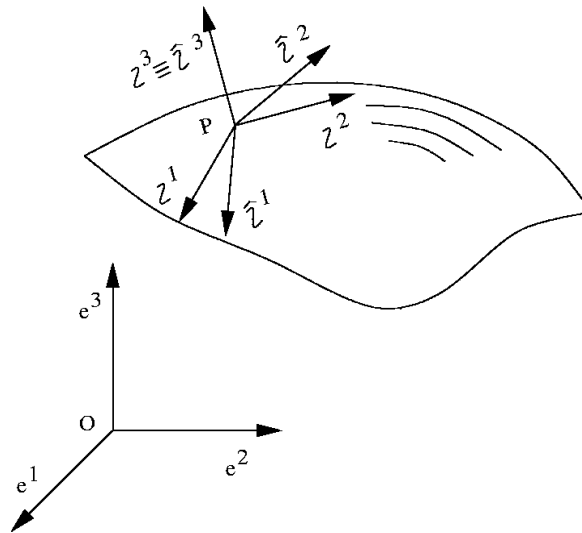


Fig. 1    Vector bases used in the finite-element model

In order to simplify the manipulation of the plane-stress condition as well as the evolution of the plastic orthotropy, two orthonormal vector bases are attached to each particle. They are denoted by $\imath^1$, $\imath^2$, $\imath^3$ and $\hat{\imath}^1$, $\hat{\imath}^2$, $\hat{\imath}^3$ in Figure 1 and change continuously during the simulation of the forming process. Both bases have two vectors tangent to the membrane surface ($\imath^1$, $\imath^2$ and $\hat{\imath}^1$, $\hat{\imath}^2$, respectively). $\imath^1$ is obtained by projecting $\mathbf{e}^1$ onto the tangent plane. In case that $\mathbf{e}^1$ is almost perpendicular to the surface of the membrane, $\imath^1$ is calculated as the projection of $\mathbf{e^3}$. The unit vector $\imath^3$ is always perpendicular to the membrane, so its construction is straightforward. At last, $\imath^2$ results as the cross product of $\imath^3$ and $\imath^1$. The vectors $\hat{\imath}^1$, $\hat{\imath}^2$ and $\hat{\imath}^3$ are respectively coincident with the local axes of plastic orthotropy in the configuration under analysis. As mentioned above, the orientation of these axes is given by the rotational component of the deformation gradient tensor. The vectors $\hat{\imath}^1$, $\hat{\imath}^2$ and $\hat{\imath}^3$ can thus be obtained using the polar decomposition theorem /17/.

The local bases are used to express the tensor components restricted by the plane-stress assumption, as well as to simplify the manipulation of the constitutive equations (see below).

The finite-element model included in ABAQUS/Standard is based on the theorem of virtual work /17/:

$$\int_{\Omega} \sigma_{\alpha\beta}\, \delta\varepsilon_{\alpha\beta}\, d\Omega = W^{ext}\left(u_i, \delta u_i\right) \tag{25}$$

where $\Omega$ is the spatial domain occupied by the sheet metal in the current configuration, $u_i\ (i=1,2,3)$ are components of the displacement vectors connecting the reference and current positions of the particles, $\delta u_i\ (i=1,2,3)$ are components of a virtual displacement field, $\sigma_{\alpha\beta}\ (\alpha,\beta=1,2)$ are non-zero components of the Cauchy stress tensor,

$$\delta\varepsilon_{\alpha\beta} = \frac{1}{2}\left( \frac{\partial\, \delta u_\alpha}{\partial\, x_\beta} + \frac{\partial\, \delta u_\beta}{\partial\, x_\alpha} \right) \tag{26}$$

is a virtual strain field, and $W^{ext}\left(u_i, \delta u_i\right)$ is the virtual work associated to the external loads. In case of a hydraulic bulging process, this work is done by the pressure acting on one face of the sheet metal:

$$W^{ext}\left(u_i, \delta u_i\right) = p \int_A n_i\, \delta u_i\, dA \tag{27}$$

where $A$ is the current area of the membrane surface loaded by the pressure p, and $n_i\ (i=1,2,3)$ are components of the unit vector perpendicular to this surface (this vector has the same orientation as the external load).

The vector components in equation (27) are expressed in the global basis $\mathbf{e}^1$, $\mathbf{e}^2$, $\mathbf{e}^3$. On the other hand, the tensor components in equation (25) are expressed in the local basis $\mathbf{i}^1$, $\mathbf{i}^2$, $\mathbf{i}^3$.

The mechanical model defined by equations (25)-(27) contains both kinematical and material non-linearities. Its solution is obtained using a Newton-Raphson procedure /17/. The linearization of equation (25) is constructed by retaining the first and second terms of its Taylor expansion in the vicinity of an approximate current configuration /17/:

$$\int_\Omega (\delta\varepsilon_{\alpha\beta}) C^{ep}_{\alpha\beta\eta\lambda} (\Delta\varepsilon_{\eta\lambda}) d\Omega - 2\int_\Omega (\delta\varepsilon_{\alpha\beta})\sigma_{\alpha\eta}(\Delta\varepsilon_{\eta\beta}) d\Omega + \int_\Omega \frac{\partial\delta u_i}{\partial x_\alpha}\frac{\partial\Delta u_i}{\partial x_\beta}\sigma_{\alpha\beta} d\Omega =$$

$$W^{ext}(u_i,\delta u_i) + \frac{\partial W^{ext}}{\partial u_i}(\Delta u_i) - \int_\Omega (\delta\varepsilon_{\alpha\beta})\sigma_{\alpha\beta} d\Omega \qquad (28)$$

where $\Delta u_i\ (i=1,2,3)$ are corrections of the displacement field components,

$$\Delta\varepsilon_{\alpha\beta} = \frac{1}{2}\left(\frac{\partial\Delta u_\alpha}{\partial x_\beta} + \frac{\partial\Delta u_\beta}{\partial x_\alpha}\right) \qquad (29)$$

are the corresponding corrections of the strain components, and $C^{ep}_{\alpha\beta\eta\lambda}\ (\alpha,\beta,\eta,\lambda=1,2)$ are components of the so-called elastoplastic modulus consistent with the Newton-Raphson scheme. This last quantity defines a relationship between the corrections of the stress and strain tensors /17/:

$$\Delta\sigma_{\alpha\beta} + \sigma_{\alpha\eta}(\Delta R_{\eta\lambda})R_{\beta\lambda} - (\Delta R_{\alpha\eta})R_{\lambda\eta}\sigma_{\lambda\beta} = C^{ep}_{\alpha\beta\eta\lambda}(\Delta\varepsilon_{\eta\lambda}) \qquad (30)$$

$R_{\alpha\beta}\ (\alpha,\beta=1,2)$ are components of the rotation tensor and $\Delta R_{\alpha\beta}\ (\alpha,\beta=1,2)$ are their corrections.

Due to the fact that all the constitutive equations discussed in §2 contain tensors expressed in the system of plastic orthotropy axes, it is more convenient to start the evaluation of the elastoplastic modulus in the co-rotational basis $\hat{\mathbf{i}}^1$, $\hat{\mathbf{i}}^2$, $\hat{\mathbf{i}}^3$. The transfer of the co-rotational components $\hat{C}^{ep}_{\alpha\beta\eta\lambda}\ (\alpha,\beta,\eta,\lambda=1,2)$ to the general basis $(\mathbf{i}^1, \mathbf{i}^2, \mathbf{i}^3)$ consists in performing the following transformation /17/:

$$C^{ep}_{\alpha\beta\eta\lambda} = R_{\alpha\omega}R_{\beta\psi}R_{\eta\varphi}R_{\lambda\xi}\hat{C}^{ep}_{\omega\psi\varphi\xi} \qquad (31)$$

The co-rotational components $\hat{C}^{ep}_{\alpha\beta\eta\lambda}\ (\alpha,\beta,\eta,\lambda=1,2)$ can be calculated using the matrix formula /17/

$$\left[\hat{C}^{ep}\right] = \left[\hat{C}^e\right] - \frac{1}{\{\hat{g}\}^T\left[\hat{C}^e\right]\{\hat{g}\}+H}\cdot\left(\left[\hat{C}^e\right]\{\hat{g}\}\right)\left(\{\hat{g}\}^T\left[\hat{C}^e\right]\right) \qquad (32)$$

where

$$\left[\hat{C}^{ep}\right]=\begin{bmatrix} \hat{C}^{ep}_{1111} & \hat{C}^{ep}_{1122} & \frac{1}{2}\left(\hat{C}^{ep}_{1112}+\hat{C}^{ep}_{1121}\right) \\ \hat{C}^{ep}_{2211} & \hat{C}^{ep}_{2222} & \frac{1}{2}\left(\hat{C}^{ep}_{2212}+\hat{C}^{ep}_{2221}\right) \\ \hat{C}^{ep}_{1211} & \hat{C}^{ep}_{1222} & \frac{1}{2}\left(\hat{C}^{ep}_{12112}+\hat{C}^{ep}_{1221}\right) \end{bmatrix} \tag{33}$$

$$\{\hat{g}\}=\left[\frac{\partial\Phi}{\partial\hat{\sigma}_{11}},\frac{\partial\Phi}{\partial\hat{\sigma}_{22}},2\frac{\partial\Phi}{\partial\hat{\sigma}_{12}}\right]^{T} \tag{34}$$

$$H=\frac{dY}{d\overline{\varepsilon}^{p}} \tag{35}$$

$$\left[\hat{C}^{e}\right]=\left([U]+\left(^{1}\overline{\varepsilon}^{p}-^{0}\overline{\varepsilon}^{p}\right)[C^{e}]\left[\hat{M}\right]\right)^{-1}[C^{e}] \tag{36}$$

The equations (34) – (36) need some explanations. The column-vector $\{\hat{g}\}$ defines the gradient of the yield surface described by equations (1) – (3). It contains the first derivatives of the function $\Phi$ with respect to the co-rotational components of the stress tensor in the current approximate configuration. $H$ is the strain-hardening modulus. It is the first derivative of the Swift hardening law with respect to the equivalent plastic strain in the current approximate configuration (see equation (8)). $^{0}\overline{\varepsilon}^{p}$ and $^{1}\overline{\varepsilon}^{p}$ are the equivalent plastic strains associated to the reference configuration and current approximate configuration, respectively. $[U]$ is the third-order unit matrix, while the other matrices used in equation (36) have the following structure:

$$\left[\hat{M}\right]=\begin{bmatrix} \dfrac{\partial^{2}\Phi}{\partial\hat{\sigma}_{11}^{2}} & \dfrac{\partial^{2}\Phi}{\partial\hat{\sigma}_{11}\partial\hat{\sigma}_{22}} & 2\dfrac{\partial^{2}\Phi}{\partial\hat{\sigma}_{11}\partial\hat{\sigma}_{12}} \\ & \dfrac{\partial^{2}\Phi}{\partial\hat{\sigma}_{22}^{2}} & 2\dfrac{\partial^{2}\Phi}{\partial\hat{\sigma}_{22}\partial\hat{\sigma}_{12}} \\ \text{symm.} & & 2\left(\dfrac{\partial^{2}\Phi}{\partial\hat{\sigma}_{12}^{2}}+\dfrac{\partial^{2}\Phi}{\partial\hat{\sigma}_{12}\partial\hat{\sigma}_{21}}\right) \end{bmatrix} \tag{37}$$

$$[C^{e}]=\frac{E}{1-\nu^{2}}\begin{bmatrix} 1 & \nu & 0 \\ \nu & 1 & 0 \\ 0 & 0 & \frac{1-\nu}{2} \end{bmatrix} \tag{38}$$ $\left[\hat{M}\right]$ is related to the curvature of the yield surface. Its

elements are the second order derivatives of the function $\Phi$ with respect to the co-rotational components of the stress tensor in the current approximate configuration. Finally, $\left[C^e\right]$ is the classical elasticity matrix for plane-stress problems. Its elements depend on the Young's modulus $E$ and the Poisson's ratio $\nu$.

The simulation of the hydroforming process is divided into small time increments. For each increment, a finite-element approximation of equation (28) is solved numerically using a Newton-Raphson procedure. After achieving the convergence, the nodal coordinates and the state parameters of the elements are updated. These parameters are the plastic equivalent strain, the thickness of the membrane and the components of the stress tensor associated to the integration points. After updating, the current configuration of the finite-element model is taken as a reference status for the next increment. The simulation is stopped when the pressure acting on the sheet metal reaches its maximum value.

## 2.7  Results and discutions

The authors have implemented the elastoplastic material model in ABAQUS/Standard by means of a UMAT subroutine. This subroutine has been used for the simulation of a hydraulic bulging test. The forming process is schematically shown in Figure 2. The mechanical parameters of the sheet metal (AA3003-0; thickness 1 mm) are listed in Table 1. The circular specimen comes into contact with the clamping ring in the region of the fillet. The frictional component of this interaction is described by the classical Coulomb model implemented in ABAQUS/Standard (a friction coefficient $\mu = 0.15$ is assigned to the contact surface). The pressure of the liquid has been used as a control parameter. Its value is considered to have a linear variation from 0 to 4 MPa.
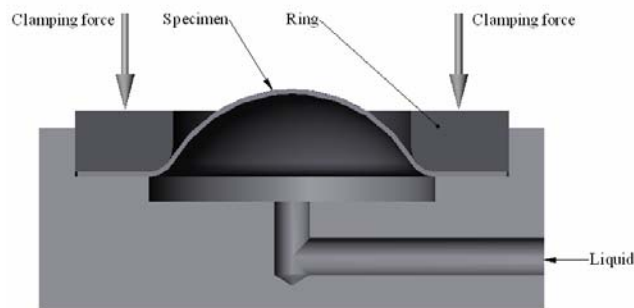


Fig. 2   Principle   of   the hydraulic bulging test

The elastic behaviour of the sheet metal is defined by the Young's modulus $E = 6.01 \times 10^4 \, \text{MPa}$ and the Poisson's ratio $\nu = 0.33$. The plastic behaviour is defined by the coefficients of the yield criterion (see Table 2) and the coefficients of the Swift hardening law: $K = 199.8 \, \text{MPa}$, $\bar{\varepsilon}^0 = 0.0056$ and $n = 0.2005$ (see equation (8)).

Due to the plastic orthotropy of the sheet metal, as well as the axial symmetry of the tools, only one quarter of the specimen needs to be meshed. The external boundary of the mesh corresponds to the clamping circle (see Figure 2). The radius of this circle is 58 mm. All the nodes belonging to the external contour are completely restrained. The fillet radius of the clamping ring is 5 mm (see Figure 2). The mesh used in the simulation consists of 18 M3D3 elements and 504 M3D4 elements /17/, with a total number of 553 nodes.

The experimental work has been performed in the Institute of Metal Forming (IFU) of the University of Stuttgart. Three specimens have been subjected to the hydraulic bulging test.

The polar deflection corresponding to different values of the liquid pressure has been recorded for each specimen. The results of these measurements are plotted in Figure 3 as discrete points. The dependence pressure vs. polar deflection predicted by the finite-element programme is superimposed on the same diagram. One may notice a very good agreement between the numerical results and the experimental data.

ABAQUS/Standard also computes the spatial distributions of the strain and stress components. A rectangular grid has been printed on each specimen. The distribution of the principal logarithmic strains at the end of the bulging test can thus be measured. Figures 4 and 5 show a comparison of the experimental and computed values of the principal logarithmic strains.

As one may notice when examining the diagrams presented in Figures 4 and 5, the predictions of the elastoplastic model are in good agreement with the data obtained from experiments. Little differences between the computed and measured values of the principal logarithmic strains appear in the vicinity of the clamping edge. The frictional effects associated to the contact interactions between the specimen and the metallic ring are probably responsible for this inaccuracy. Another cause of the discrepancies may be the errors of the strain measurements in the clamping region (due to the high curvature of the sheet metal specimen at the end of the forming process).
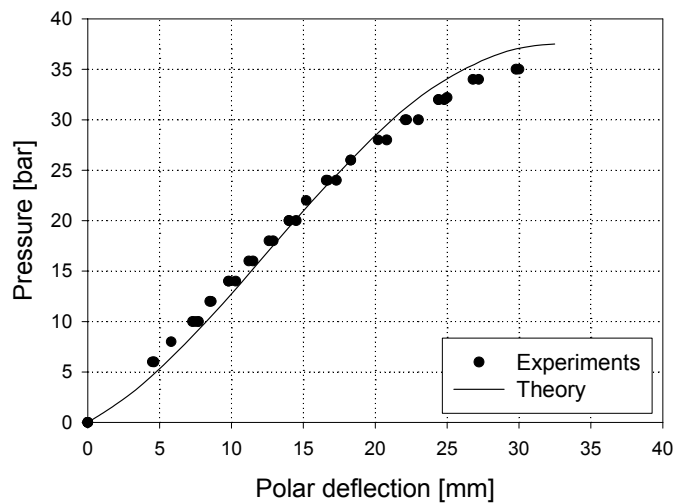
Fig. 3    Pressure vs. polar deflection (comparison between
          numerical results and experimental data
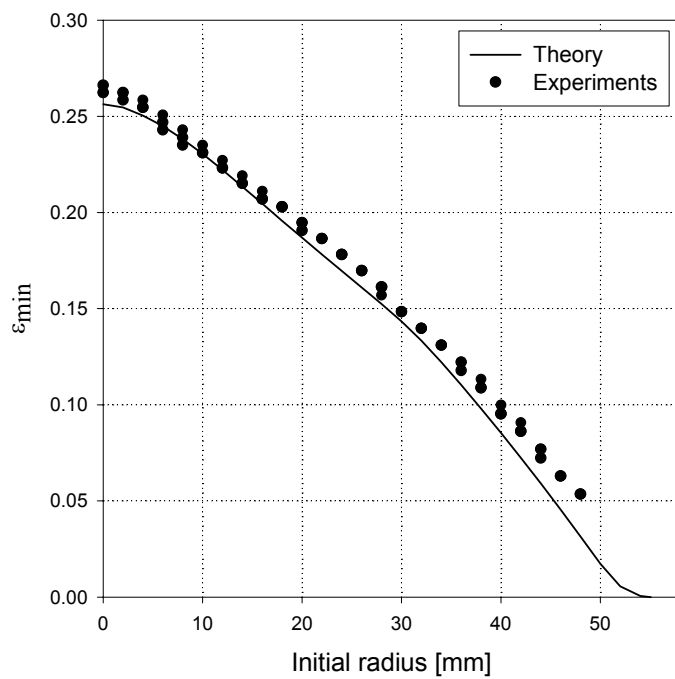


Fig. 4    Computed and experimental distributions of the minor principal
          logarithmic strain at the end of the bulging test
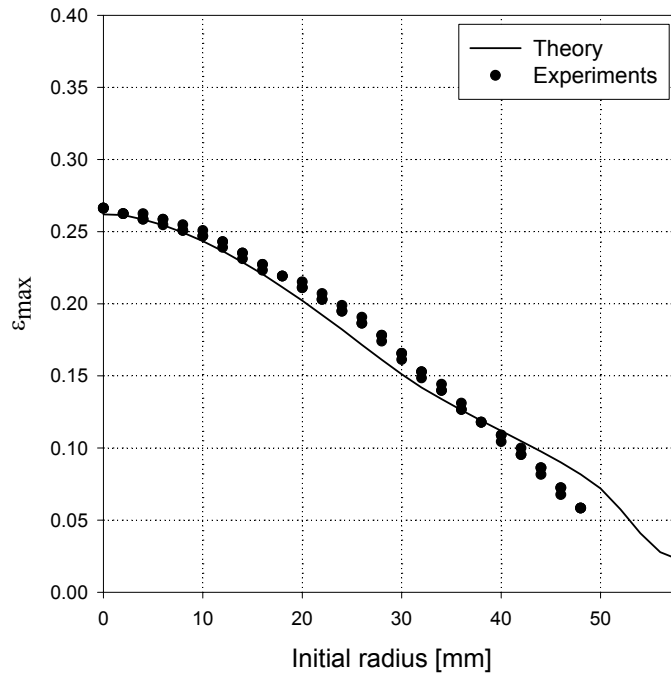
Fig. 5    Computed and experimental distributions of the major principal
          logarithmic strain at the end of the bulging test

## 3  Conclusions

The hydraulic bulging test is particularly suitable for studying the mechanical response of sheet metals subjected to biaxial loads. The authors have used this test to evaluate the performances of a new yield criterion. The equibiaxial yield stress of the sheet metal is one of the parameters used in the identification procedure. Due to the close relation between this parameter and the mechanics of the hydraulic bulging process, the new yield criterion gives accurate predictions. The distributions of the principal logarithmic strains resulted from computations are in very good agreement with experimental data. The authors have noticed that the accuracy of the pressure vs. polar deflection curve is highly influenced by the hardening rule used in the model.

## References

/1/     Hill, R.              The Mathematical Theory of Plasticity
                             Oxford: Clarendon Press, 1950


/2/     Hill, R.              Theoretical plasticity of textured aggregates
                             In: Math. Proc. Cambridge Phil. Soc. 85 (1979) 179


/3/     Hill, R.              Constitutive modelling of orthotropic plasticity in sheet
                             metals
                             In: J. Mech. Phys. Solids 38 (1990) 405

/4/     Hill, R.              A user-friendly theory of orthotropic plasticity in sheet
                             metals
                             In: Int. J. Mech. Sci. 35 (1993) 19

/5/     Hosford, W. F.       A generalized isotropic yield criterion
                             In: J. Appl. Mech. 39 (1972) 607

/6/     Hosford, W. F.       On yield loci of anisotropic cubic metals
                             In: Proc. 7th North American Metalworking Conf.-
                             Dearborn (1979) 191

/7/     Barlat, F.           Plastic behavior and stretchability of sheet metals. Part I:
        Lian, J.             Yield function for orthotropic sheets under plane stress
                             conditions
                             In: Int. J. Plasticity 5 (1989) 51

/8/     Barlat, F.           A six-component yield function for anisotropic materials
        Lege, D. J.          In: Int. J. Plasticity 7 (1991) 693
        Brem, J. C.

/9/     Barlat, F.           Yield function development for aluminium alloy sheets
        Lege, D. J.          In: J. Mech. Phys. Solids 45 (1997) 1727
        Matsui, K.
        Murtha, S. J.
        Hattori, S.
        Becker, R.C.
        Makosey, S.

/10/    Barlat, F.           Plane stress yield function for aluminium alloy sheets. Part
        Brem, J. C.          I: Formulation

|  |  | Yoon, J. W. | In: Int. J. Plasticity (to be published) |
|  |  | Chung, K. |  |
|  |  | Dick, R. E. |  |
|  |  | Lege, D. J. |  |
|  |  | Pourboghrat, F. |  |
|  |  | Choi, S. H. |  |
|  |  | Chu, E. |  |

/11/ Karafillis, A. P. — A general anisotropic yield criterion using bounds and a  
     Boyce, M. C. — transformation weighting tensor  
     In: J. Mech. Phys. Solids 41 (1993) 1859

/12/ Cazacu, O. — Application of the theory of representation to describe  
     Barlat, F. — yielding of anisotropic aluminum alloys  
     In: Int. J. Engng Sci. (to be published)

/13/ Banabic, D. — Formability of Metallic Materials. Plastic Anisotropy,  
     Bunge, H. J. — Formability Testing, Forming Limits  
     Poehlandt, K. — Berlin: Springer Verlag, 2000  
     Tekkaya, A. E.

/14/ Lemaître, J. — Mécanique des matériaux solides  
     Chaboche, J. L. — Paris: Dunod, 1988

/15/ Press, W. H. — Numerical Recipes in C. The Art of Scientific Computing  
     Teukolsky, S. H. — Cambridge: Cambridge University Press, 1992  
     Vetterling, W. T.  
     Flannery, B. P.

/16/ Vial, C. — Yield loci of anisotropic sheet metals  
     Hosford, W. F. — In: Int. J. Mech. Sci. 25 (1983) 899  
     Caddell, R. M.

/17/ ABAQUS, Inc. — ABAQUS Theory Manual. Version 6.2.3  
     Electronic documentation